

**RERTR 2011 — 33rd INTERNATIONAL MEETING ON
REDUCED ENRICHMENT FOR RESEARCH AND TEST REACTORS**

**October 23-27, 2011
Marriott Santiago Hotel
Sandiago, Chile**

**RECENT DEVELOPMENT IN TEM CHARACTERIZATION OF
IRRADIATED RERTR FUELS**

J. Gan, B.D. Miller, D.D. Keiser Jr., A.B. Robinson, J.W. Madden,
P.G. Medvedev and D.M. Wachs

Nuclear Fuels and Materials Division
Idaho National Laboratory, P.O. Box 1625, Idaho Falls, ID 83415, USA

ABSTRACT

The recent development on TEM work of irradiated RERTR fuels includes characterization of the irradiated U-10Mo/Alloy-6061 monolithic fuel plate, the RERTR-7 U-7Mo/Al-2Si and U-7Mo/Al-5Si dispersion fuel plates. It is the first time that a TEM sample of an irradiated nuclear fuel was prepared using the focused-ion-beam (FIB) lift-out technical at the Idaho National Laboratory. Multiple FIB TEM samples were prepared from the areas of interest in a SEM sample. The characterization was carried out using a 200kV TEM with a LaB₆ filament. The three dimensional orderings of nanometer-sized fission gas bubbles are observed in the crystalline region of the U-Mo fuel. The co-existence of bubble superlattice and dislocations is evident. Detailed microstructural information along with composition analysis is obtained. The results and their implication on the performance of these fuels are discussed.

1. INTRODUCTION

The microstructural characterization using transmission electron microscopy (TEM) for the irradiated fuel plates of the research and test reactor fuels played an important role to the understanding of fuel performance. Significant progresses have been made over the last several years on TEM work for the program on fuel development for reduced enrichment for research and test reactors (RERTR) [1, 2]. For the post irradiation examination of the irradiated fuel plate, it is important to carry out a full characterization of microstructure at different scale: Optical microscopy, electron probe micro-analysis (EPMA), scanning electron microscopy (SEM) and TEM. This allows capturing the complete microstructural features responsible for the fuel behavior in a reactor.

While many research and test reactors can use dispersion fuels with low enrichment ($^{235}\text{U} < 20 \text{ at.\%U}$), certain type of high performance reactors have to use monolithic fuel plate to replace the dispersion fuel plate because the former allows higher fuel loading in term of $^{235}\text{U}/\text{cm}^3$ in the fuel. The microstructural characterization with TEM for the irradiate fuel plate is crucial to provide nanometer scale details on fission product distribution, fission gas bubble morphology, fuel-cladding interaction and the microstructural and composition changes as a results of fissions and fast neutrons. Sample preparation for TEM analysis of an irradiated monolithic fuel imposes additional challenges comparing to that of an irradiated dispersion fuel because the small punch fuel specimen can not be produced.

A pioneer work on TEM sample preparation of irradiated nuclear fuel using focused ion beam (FIB) lift-out technique has been explored successfully at the Idaho National Laboratory in the USA. Using a focused Ga ion beam in FIB, samples can be produced with a typical size of $10 \times 15 \mu\text{m}^2$ and an appropriate thickness ($< 100 \text{ nm}$) transparent to the 200keV electron beam for TEM analysis. From a SEM sample, the areas of interest can be identified such as fuel-cladding-interaction (FCI) layer, middle of fuel zone and various phases and features. Multiple FIB-TEM samples can be produced from these areas. These FIB-TEM samples can provide site-specific local microstructure information otherwise unreachable through sample prepared conventionally. FIB lift-out sample eliminates the surface smear and provides much better surface condition for SEM characterization than sample prepared from mechanical polishing. Another major advantage of using FIB-TEM sample for the irradiated fuel is its significantly reduced activity due to very small sample volume, therefore improving analytical measurement with the Energy Dispersive Spectroscopy (EDS). However, since the area covered by a FIB sample is quite small comparing to a conventional TEM disc sample, multiple FIB-TEM samples are required to capture the entire microstructure.

This work will report the first TEM characterization of the irradiated monolithic fuel samples prepared using FIB lift-out technique. In addition, the result from a FIB-TEM sample cut from the middle of a fuel particle in U-7Mo/Al-2Si dispersion fuel and preliminary results from a U-7Mo/Al-5Si dispersion fuel plate are also present.

2. EXPERIMENTS

The monolithic fuel plate (L1F140) with U-10Mo fuel and Al alloy 6061 cladding was fabricated using 250 μm fuel foil and friction bonding. It was irradiated in the Advanced Test Reactor (ATR) at INL to an average fission density of $5.25 \times 10^{27} \text{ f/m}^3$ calculated using a PLATE fuel performance code [3]. A small piece of monolithic fuel was sliced off the irradiated fuel plate at the Hot Fuel Examination Facility (HFEF) at INL. This sample has a total activity comparable to that of the small 1.0 mm diameter punch sample of the dispersion fuel plate. The estimated local fission density, fission rate and fuel plate centerline temperature for the monolithic fuel is $3.46 \times 10^{27} \text{ f/m}^3$, $4.45 \times 10^{20} \text{ f/m}^3\text{-s}$ and 112°C , respectively. TEM samples were prepared at the Electron Microscopy Laboratory (EML). A dual beam FEI Quanta3D FIB/SEM system was used for FIB-TEM sample lift-out, thinning and SEM imaging. TEM characterization was carried out using a 200 kV JEOL-2010 microscope with a LaB₆ filament.

A schematic of FIB-TEM sample preparation is shown in Fig. 1 where a SEM sample was first prepared and characterized, followed by FIB lift-out from the specific areas, SEM imaging of the lift-out sample, final thinning of the FIB lift-out sample for TEM characterization. The FIB-TEM sample from the middle of a dispersion fuel particle in a U-7Mo/Al-2Si SEM sample was prepared following the same

fashion. The estimated local fission density and the irradiation temperature for the dispersion fuel is $6.31 \times 10^{27} \text{ f/m}^3$ and 120°C , respectively. For the irradiated U-7Mo/Al-5Si dispersion fuel plate, a TEM sample was prepared using a 1.0 mm diameter fuel punch. The details on sample preparation can be found in the reference [2]. The local fission density and irradiation temperature is estimated to be $5.16 \times 10^{27} \text{ f/m}^3$ and 130°C , respectively. Only the preliminary result for this sample is reported here.

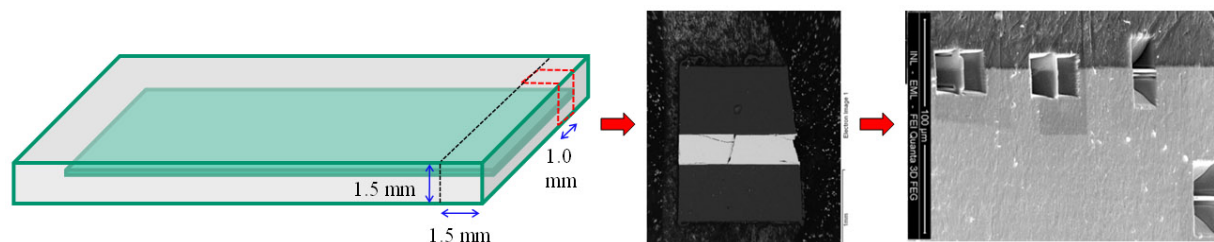


Figure 1. Schematic of sample preparation from an irradiated monolithic fuel plate by slicing of an irradiated fuel plate (left), SEM sample mounting (middle), FIB trenching and lift-out (right) followed by final ion milling for TEM characterization.

3. RESULTS AND DISCUSSIONS

An SEM high magnification image of the TEM lamella before final thinning and a TEM low magnification image of the TEM lamella after final thinning are shown in Figure 2 for an irradiated monolithic U-10Mo/Al 6061 fuel plate. The SEM image reveals the fission gas bubble distribution and morphology near the fuel-cladding interface. On the fuel side (light contrast) in the right, these bubbles reside at the grain boundary with irregular shapes. In area with still light contrast next to the interface in the fuel, circular bubbles are present indicating the material within this narrow zone turn to amorphous. The area with dark grey contrast next to the Al 6061 cladding (dark contrast) is the fuel-cladding interaction (FCI) layer which is amorphous. The low magnification TEM image reveals the grain boundary bubbles from a different area. The inclined light contrast streaks, an indication of thinner areas, are the artifact from FIB ion polishing as a result of the fixed ion beam direction.

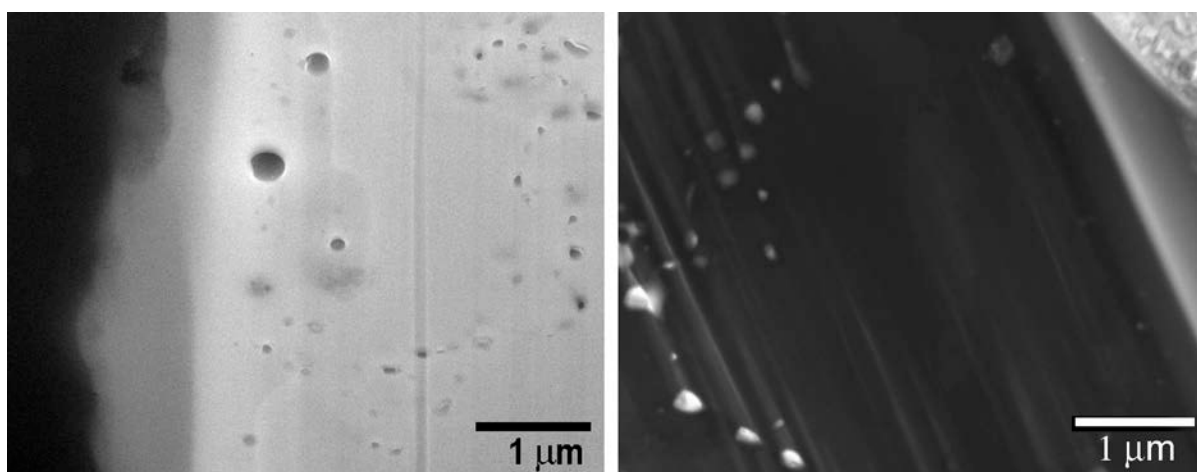


Figure 2. SEM image (left) of FIB lift-out showing bubbles in FCI layer and at grain boundary in fuel, and a low magnification TEM image (right) showing grain boundary bubbles.

A bright field TEM image in Figure 3 shows more detailed microstructure at FCI layer from fuel (left) to cladding (right). The composition data from energy dispersive spectroscopy (EDS) measurements for the marked spots are listed in Table 1. Note the composition changes from A, B to C, D with a drop in U by ~ 20 at% and the presence of high Si (~ 16 at% Si) for the latter. The narrow region marked by C and D was identified as amorphous with composition significantly different from that of a typical FCI layer. The similar amorphous zone with high U, Mo and Si was also found in the fuel particles in irradiated dispersion fuel plate. The size of this amorphous zone can be several microns. As it clearly shows in Table 1, there is no deep penetration of Si into U-Mo fuel. The Mg rich precipitates in FCI layer near the cladding side are likely the result of segregation of Mg in Al 6061 into the FCI and cladding interface. Since no diffraction spots can be identified from the convergent beam micro diffraction analysis, these Mg rich precipitates are likely amorphous. Note that both Si and Mg are present in Al 6061 composition.

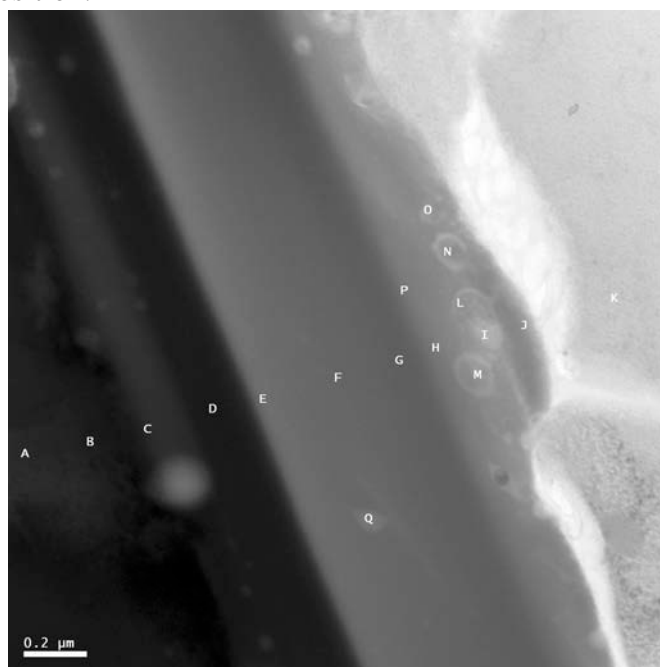


Figure 3. TEM image showing microstructure across the fuel-cladding interaction layer with composition measurement from EDS.

Table 1. EDS measurement (at.%) at spots marked in Figure 3.

Spot	U	Si	Al	Mo	Other	Note
A	75	0.6	1.9	23		Fuel, Si ~ 0, crystalline
B	77	0	3.4	25		Fuel, Si ~ 0, crystalline
C	57	14	3.4	25		Fuel, high Si, amorphous
D	55	18	7.1	20		Fuel, high Si, amorphous
E	14	1.7	78	6.4		FCI, low Si, amorphous
F	13	3.3	77	6.6		FCI, low Si, amorphous
G	14	7.0	75	4.9		FCI, low Si, amorphous
H	13	6.3	77	4.5		FCI, low Si, amorphous
I	7.1	1.9	72	4.0	Mg_16	Mg rich precipitates
J	8.7	4.4	76	2.5	Mg_8.1	Mg rich precipitates
K	0.1	0	99.9	0		Al 6061 cladding, crystalline
L	8.6	4.5	72	3.8	Mg_11	Mg rich precipitates
M	7.9	3.6	73	3.6	Mg_12	Mg rich precipitates

N	8.9	5.9	71	3.4	Mg_8.9	Mg rich precipitates
O	9.0	4.6	70	4.1	Mg_12	Mg rich precipitates
P	12	6.4	74	4.3	Mg_2.9	Mg rich precipitates
Q	13	2.5	77	7.0		FCI, low Si, amorphous

In the fuel zone of the irradiated monolithic fuel plate, bubble superlattice is observed as shown in Fig. 4 at two different magnifications. It was identified that this bubble superlattice has fcc structure coherent to the bcc structure of U-Mo. The images on the right show the selected area diffraction (SAD) patterns at zone [100] at two different camera lengths with the bottom one showing the detail of the SAD spots.

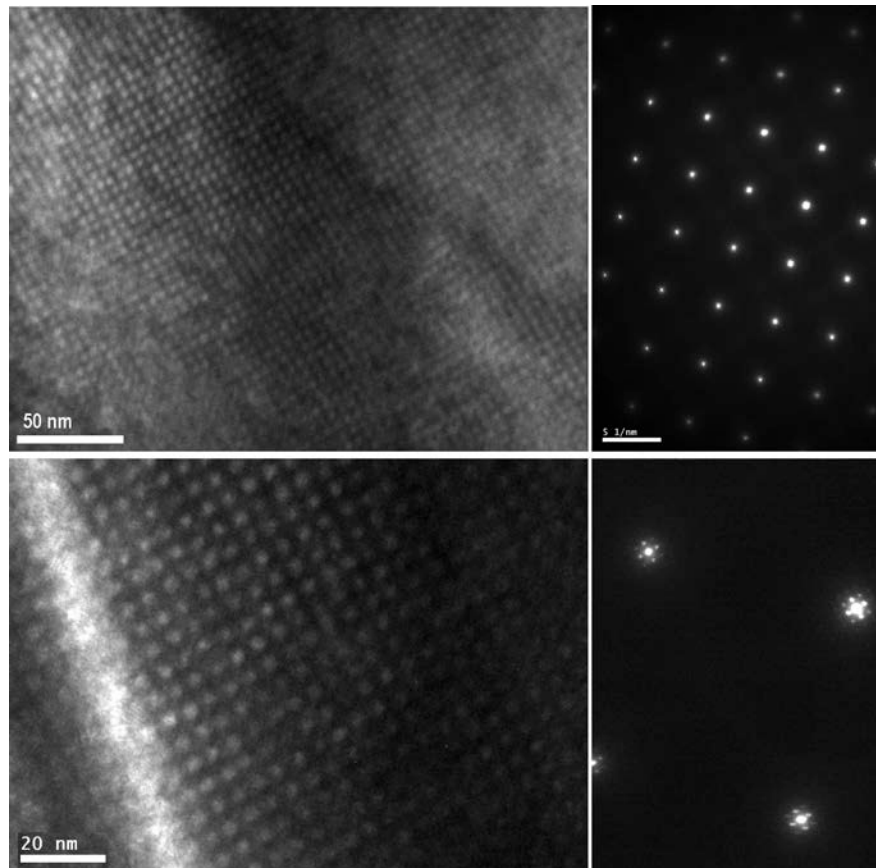


Figure 4. TEM images of Bubble superlattice in the irradiated U-10Mo fuel imaged at zone [100] at low mag. (low-left) and high mag. (up-left) with SAD pattern (low-right) and a magnified view (up-right) showing satellite spots from bubble superlattice.

A low magnification bright-field TEM image (Fig. 5, left) shows both bubble superlattice near zone [011] and dislocations ($g=200$). It appears that the effect of dislocations on the development and the stability of the bubble superlattice is negligible. These dislocations are likely the results of both heavy cold work ($\sim 90\%$) in the U-10Mo fuel foil before fuel plate fabrication and the radiation induced microstructural damage. A high magnification TEM image (Fig. 5, right) shows superlattice bubbles near a large bubble located at grain boundary. It clearly shows that superlattice bubbles remain stable at a distance as close as ~ 70 nm from the grain boundary bubbles at the fission density of 3.4×10^{27} fissions/ m^3 in U-10Mo. This property is important to maintain good fuel performance at high fission densities.

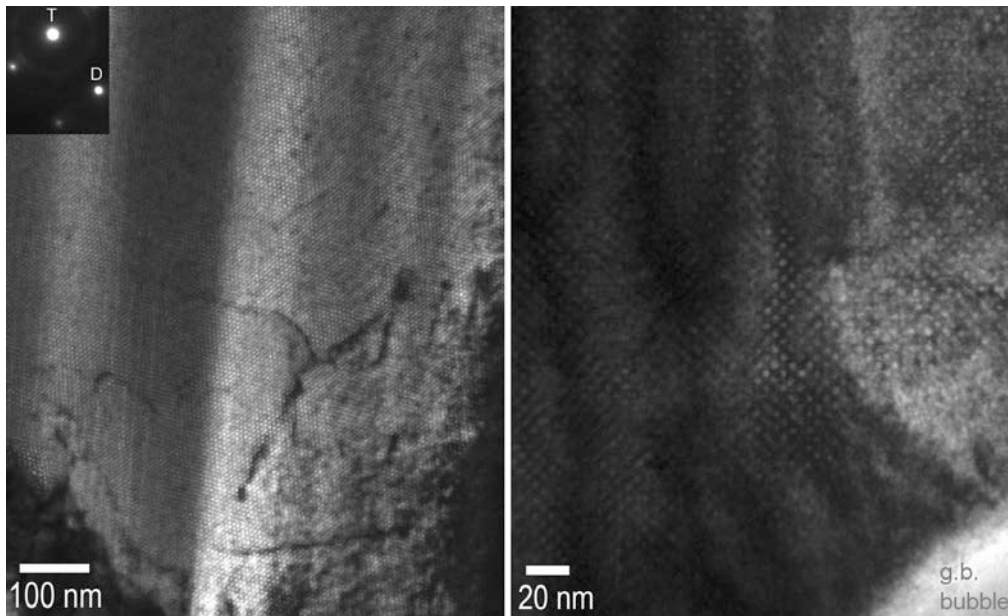


Figure 5. Low mag. TEM image (left) showing bubble superlattice (zone [110]) and dislocations ($g=200$, see inset) and a high mag. TEM image (right) showing superlattice bubbles (zone [100]) near a grain boundary bubble (low right).

As a part of TEM characterization development for irradiated fuels using FIB, a FIB lift-out sample from an U-7Mo/Al-2Si dispersion fuel SEM sample irradiated to high fission density ($6.3 \times 10^{27} \text{ f/m}^3$) was also prepared and shown in a SEM image in Fig. 6. It provides exceptional details at the fuel-cladding interface. Note that the SEM information revealed in this FIB lift-out sample is not accessible from a conventionally prepared SEM sample because the mechanical polishing induces surface smear that either changes or removes these microstructural features. The arrows indicate the beginning of interlink between the large bubbles. The image clearly shows the distribution of the large bubbles and the morphology of these bubbles with circular shape in amorphous region and irregular shape in crystalline region as a result of surface energy dependence on the structure. Preferential association of solid fission product precipitate to the large bubble is clearly demonstrated.

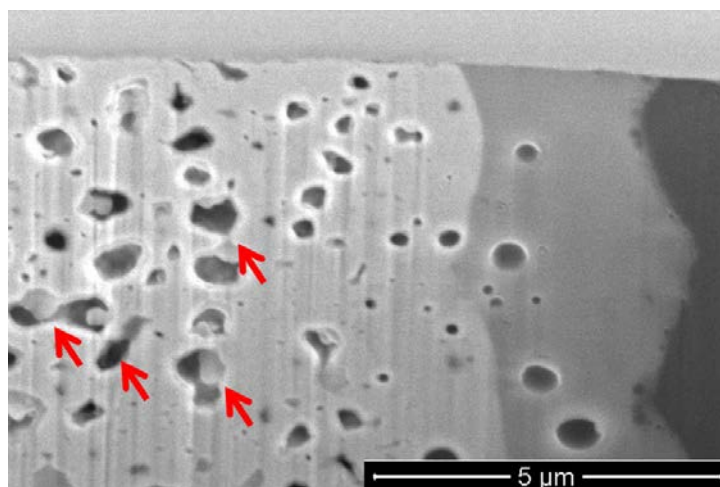


Figure 6. SEM image of a FIB-TEM lift-out specimen for an irradiated dispersion fuel showing bubble distribution and morphology in a fuel particle (left, light contrast), FMI (grey contrast) and Al-2Si matrix (right, dark contrast). Arrows showing evidence of the early stage bubble inter-link.

After final ion thinning of the lift-out sample in a FIB, a low magnification TEM image revealing the irradiated microstructure around the fuel-cladding interface is shown in Fig. 7. It shows Al alloy cladding (A), FMI (B-D), high Si amorphous fuel region (E-F), crystalline fuel region (G-K) and solid fission product precipitates (L1-L5, M1 and Z1). The mark indicates the spot where composition measurement was performed using energy dispersive spectroscopy (EDS). The results are listed in Table 2. There is no indication of Si deep penetration into the fuel since the Si content in the crystalline region of the fuel is nearly zero. It is found that area surround the large bubble turns to amorphous likely a result of fission product accumulation which significantly changes its local composition.

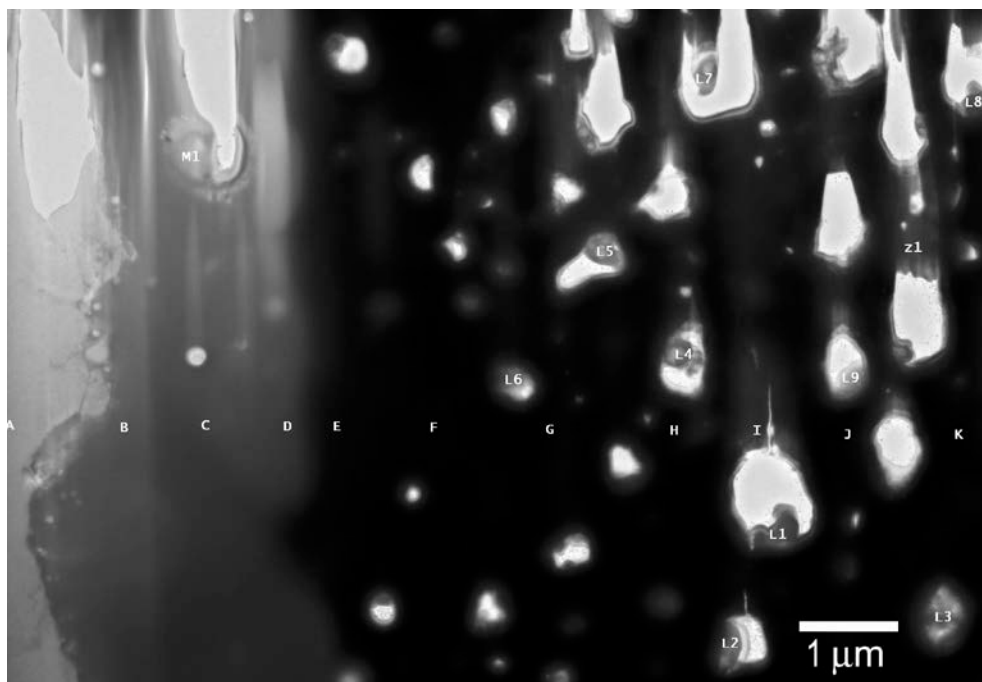


Figure 7. Low mag. TEM image of an irradiated dispersion fuel (U-7Mo/Al-2Si) showing bubble morphology and distribution in Al-2Si matrix (left, light contrast), FMI (grey contrast) and fuel particle (right, dark contrast). The EDS data of the marked areas are listed in Table 2.

Table 2. EDS measurement (at.%) of areas marked in Figure 7

Spot	U	Si	Al	Mo	Other
A	0.0	0.1	99.5	0.3	Al alloy
B	12	13	71	3.4	Fuel-Matrix Interaction (FMI)
C	14	3.5	79	4.0	FMI
D	17	1.1	77	1.1	FMI
E	61	5.3	18	15	High Si layer (amorphous)
F	67	11	5.3	17	High Si layer (amorphous)
G	82	1.5	0.0	17	Fuel
H	79	1.0	1.1	19	Fuel
I	75	2.2	3.9	19	Fuel
J	81	1.1	0.7	18	Fuel
K	81	0.0	1.4	18	Fuel
L1	5.2	0.1	1.3	1.7	Sr_28, Y_23, Ba_17, Zr_9
L2	2.5	0.0	1.0	0.9	Sr_37, Y_17, Ba_30, Zr_6
L3	5.2	0.0	5.9	1.8	Sr_31, Y_14, Ba_29, Zr_7

L4	13	0.0	1.3	5.8	Sr_30, Y_16, Ba_19, Zr_7
L5	5.2	0.0	1.2	1.4	Sr_31, Y_18, Ba_23, Zr_10
L6	67	0.0	1.8	24	Zr_4.9
L7	43	0.0	2.5	21	Sr_1, Y_3, Nd_21, Zr_3
L8	7.5	0.0	0.0	5.1	Sr_36, Y_22, Ba_14, Zr_9, Ba_14, Nd_2,
M1	13	0.0	61	2.9	Sr_2, Zr_21 (FMI)
Z1	77	0.7	1.5	17	Zr_3 (Crystalline)

A high magnification TEM image of U-7Mo fuel particle is shown in Fig. 8. The arrow indicates a small area where bubble superlattice is still evident. However at this high fission density, there are crystalline fuel regions where bubble superlattice cannot be identified. It seems that at fission density greater than $\sim 6.0 \times 10^{27} \text{ f/m}^3$, bubble superlattice start to collapse as a result of significant microstructural damage from irradiation and composition change from fission. Another important feature captured in Fig 8 is the formation of fine grains of $\sim 150 \text{ nm}$. This may be called grain subdivision which is very similar to that observed in the high burn-up “rim” region of the UO_2 fuel pellet. To author’s knowledge, this microstructural development in U-Mo fuel has not been reported before in the open literature. Note that this grain subdivision is different from the grain recrystallization observed by others for the irradiated U-Mo fuel that is typically completed below a fission density of $3 \times 10^{27} \text{ f/m}^3$ with a resultant grain size of few μm [4-7]. As it clearly shows in Fig. 8, the grain boundaries of these fine grains are not decorated with bubbles, contrast to that of recrystallized grains where the grain boundaries are decorated with large bubbles (see Fig. 2 right).

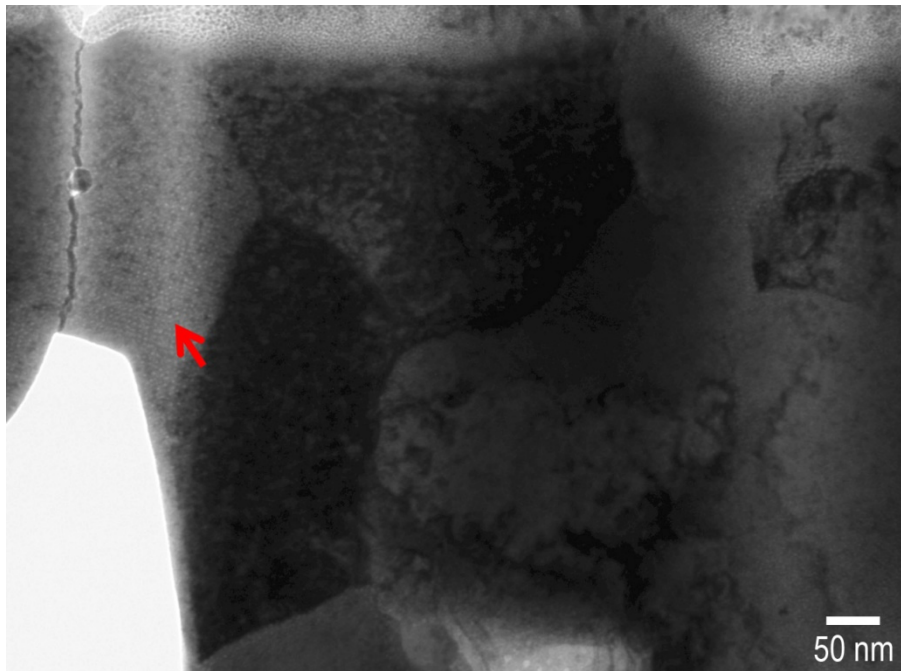


Figure 8. TEM image of an irradiated dispersion fuel (U-7Mo/Al-2Si) reveals grain subdivision and area with bubble superlattice ([100]) indicated by the arrow.

The latest TEM result is from a U-7Mo/Al-5Si high flux sample with a fission density of $5.16 \times 10^{27} \text{ f/m}^3$ with its local irradiation temperature of 130 °C. The microstructure characterization is still in the process. The preliminary result is highlighted in Fig. 9 showing bubble superlattice imaged at zone [110] at low and high magnifications. The average size of these fine bubbles is estimated to be 3.6 nm with its fcc superlattice constant of 12.0 nm. More complete characterization results will be published elsewhere.

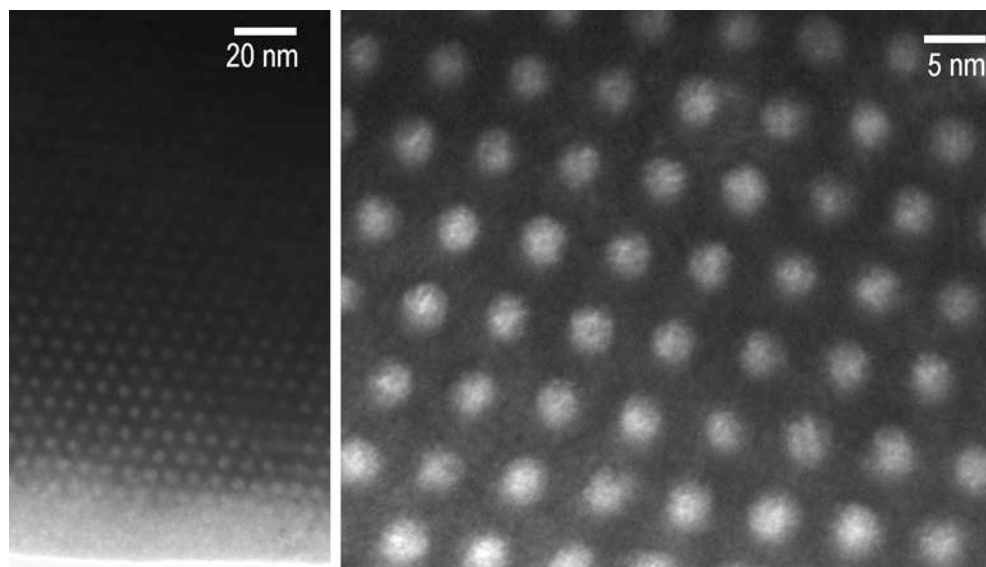


Figure 9. TEM images of an irradiated dispersion fuel (U-7Mo/Al-5Si) particle reveal superlattice bubbles (zone [110]) at relatively low mag. (left) and high mag. (right).

4. CONCLUSIONS

The TEM sample prepared using Focused-Ion-Beam technique has significant advantages over the conventionally prepared disc samples for microstructure characterization. FIB lift-out sample of the irradiated fuel can provide SEM information with undisturbed microstructure features that is not accessible from conventionally prepared SEM sample. The development of irradiated microstructure in the U-Mo fuel between the dispersion fuel and monolithic fuel plate is very similar under the relevant irradiation condition. At fission density of $5.16 \times 10^{27} \text{ f/m}^3$ or below, the bubble superlattice dominates the microstructure in the crystalline fuel. A thin layer of Si enriched fuel zone turns amorphous for both dispersion and monolithic fuel. At fission density greater than approximately $6.0 \times 10^{27} \text{ f/m}^3$, the bubble superlattice starts to collapse along with the development of grain subdivision into grains a few hundred nanometers in size.

Acknowledgements

The authors would like to express their gratitude to Paul Lind et al. HFEF staffs at INL for producing the TEM punching and cut samples. This work was supported through funding provided by the U.S. Department of Energy (DOE) to the RERTR program at Idaho National Laboratory, operated by Battelle Energy Alliance, LLC, under DOE Idaho Operations Office Contract DE-AC07-05ID14517.

U.S. Department of Energy Disclaimer

This information was prepared as an account of work sponsored by an agency of the U.S. Government. Neither the U.S. Government nor any agency thereof, nor any of their employees, makes any warranty, express or implied, or assumes any legal liability or responsibility for the accuracy, completeness, or usefulness of any information, apparatus, product, or process disclosed, or represents that its use would not infringe privately owned rights. References herein to any specific commercial product, process, or service by trade name, trademark, manufacturer, or otherwise, does not necessarily constitute or imply its endorsement, recommendation, or favoring by the U.S. Government or any agency thereof. The views and opinions of authors expressed herein do not necessarily state or reflect those of the U.S. Government or any agency thereof.

5. REFERENCES

- ¹ S. Van de Berghe, W. V. Renterghem, A. Leenaers., J. Nucl. Mater., 375 (2008) 340-346.
- ² J. Gan, D.D. Keiser Jr., D.M. Wachs, A.B. Robinson, B.D. Miller, T.R. Allen, J. Nucl. Mater., 396 (2010) 234.
- ³ Y. S. Kim, H. J. Ryu, G. L. Hofman, S. L. Hayes, M. R. Finley, D. M. Wachs, G. S. Chang, RERTR 2006, Cape Town, South Africa, http://www.rertr.anl.gov/RERTR28/PDF/S15-1_Kim.pdf
- ⁴ J. Rest, G.L. Hofman, Mat. Res. Soc. Symp. Proc. 650 (2001) R1.7.1.
- ⁵ J. Rest, J. Nucl. Mater. 326 (2004) 175-184.
- ⁶ J. Rest, J. Nucl. Mater. 346 (2005) 226-232.
- ⁷ G.L. Hofman, Y.S. Kim, Nucl. Eng. Technol. 37 (4) (2005) 299-308.